PHYSICAL REVIEW B **87**, 161202(R) (2013)

Accurate determination of homogeneous and inhomogeneous excitonic broadening in ZnO by linear and nonlinear spectroscopies

E. Mallet,[1,2,*] P. Disseix,[1,2] D. Lagarde,[3] M. Mihailovic,[1,2] F. Réveret,[1,2] T. V. Shubina,[4] and J. Leymarie[1,2]

[1]*Clermont Université, Institut Pascal (IP), BP 10448, F-63000 CLERMONT-FERRAND, France*

[2]*CNRS, UMR 6602, IP, F-63171 Aubière, France*

[3]*LPCNO, 135 avenue de Rangeuil, 31077 Toulouse Cedex, France*

[4]*Ioffe Physical-Technical Institute of RAS, St. Petersburg 194021, Russia*

(Received 11 February 2013; published 23 April 2013)

Excitonic parameters of ZnO have been determined from 5 to 300 K using the combination of time-integrated four-wave mixing, continuous wave reflectivity, autocorrelation of reflectivity at the femtosecond scale, and photoluminescence spectroscopy. These techniques allow an accurate determination of both inhomogeneous and homogeneous linewidths, oscillator strength, and other parameters characteristic for excitonic resonances. It turns out that, due to impurity-exciton scattering, the homogeneous damping of A and B excitons (0.55 and 1.35 meV, respectively) predominates over inhomogeneous one in high-quality ZnO at low temperature. Our data also prove that the strong exciton-phonon coupling enhances the excitonic broadening at room temperature up to 47 meV. This approach, which combines various sophisticated spectroscopy experiments, can be employed for an accurate determination of excitonic parameters in other semiconductor compounds and in any system where excitons are confined.

DOI: 10.1103/PhysRevB.87.161202 PACS number(s): 78.20.−e, 71.35.−y, 42.65.Re, 78.47.nj

Zinc oxide is one of the most promising semiconductors for devices emitting in the near UV.[1–3] Moreover, from a fundamental point of view, due to its large exciton binding energies and oscillator strengths, it is considered as an interesting material to observe quantum degeneracy at room temperature (RT) in microcavity structures.[4] In this context, an in-depth understanding of the ZnO exciton-polariton properties is essential for technological applications such as ultrafast micro-optical amplifiers or polaritons light emitters,[5,6] because these intrinsic properties play a key role in the device operation.

For six decades, properties of bulk ZnO have been intensively studied. They are connected to the photoluminescence (PL) emission,[7,8] the phonons,[9] the excitonic parameters,[8,10,11] and transition broadenings.[12,13] Some of them are precisely established, while others, such as the valence bands ordering[14–16] and the role of the excitons in room-temperature lasing,[17,18] have been discussed during long time. One of the controversial issues is the estimation of the exciton-polariton damping parameters that control the performance of polaritons at different temperatures. In ZnO, they have been studied at low[8,11,13] and elevated[17] temperatures, being considered as a rule in terms of homogeneous damping. However, it is necessary to make a distinction between the homogeneous damping of an excitonic resonance, Γ, and an effective damping parameter which, in fact, has been reported in the most of these papers. The first one characterizes the decay of the coherence for the localized excitation or the dephasing relaxation for exciton-polaritons.[19] In a perfect sample, it depends mostly on the interaction of the excitonic resonance with phonons. The physical meaning of the effective damping parameter is not so distinct. It is determined by many inhomogeneous factors, such as local fluctuation of strain, electric fields, etc. This is a reason to separate homogeneous and inhomogeneous parts of the damping constant so as to consider their physical origin. The knowledge of the exciton-phonon interaction is essential for the design of devices such as microcavities working at RT.

Several reasons explain the difficulties to determine the excitonic characteristics from spectroscopic measurements. That is why the combination of various spectroscopic tools and their proper choice appear to be essential. From the literature, where only one technique is generally employed, it clearly appears that the ZnO excitonic parameters aren't consistent in the whole. In particular, the broadening process at low temperature is still not well understood and the homogeneous linewidths reported at RT depend on the spectroscopy techniques that have been used.[12,13,20] A poor quality of the sample may also affect the determination of the excitonic parameters: ZnO of high quality provides, indeed, accurate values. Furthermore, time-integrated four-wave mixing (Ti-FWM) studies appear to be a prominent way to investigate the broadening transition processes[21] and to lead to a reliable determination of the exciton-phonon coupling values.

In this paper, we propose an extended experimental study of the excitonic parameters using Ti-FWM studies, continuous wave reflectivity (CW-R), autocorrelation reflectivity at the femtosecond scale (AR), and PL spectroscopy. All measurements were done in the back-scattering experimental geometry. The complementary analysis of the results obtained at 5 K by each of these methods allows homogeneous and inhomogeneous broadenings, oscillator strengths and excitonic energies to be deduced with accuracy. Exciton-phonon interaction is then determined from the association of CW-R and Ti-FWM results as a function of temperature.

As the ZnO bulk samples supplied by Tokyo Denpa Co have been grown along *c* axis, only A and B exciton could be observed according to the selection rules.[15] CW-R was performed under normal incidence from 5 K to RT using a xenon lamp for excitation. The degenerate Ti-FWM experiments are performed in backscattering configuration. The second-harmonic beam of a femtosecond Ti:sapphire laser with an adjustable pulse duration in the range of 110 to 230 fs and 76-MHz repetition rate is used to excite resonantly the

A and B excitons. The nonlinear signal is detected from a silicon photodiode with a slow response time. The AR setup uses the same laser source, the detector, and a Michelson interferometer.[22] Two collinear femtosecond pulses delayed by a time interval τ are sent on the sample at the same frequency nearly resonant with the A and B exciton transitions. Two reflected signals, with an amplitude r_g, interfere to provide the AR signal. The intensity of the time-integrated signal is then given by[22]

$$I_{\mathrm{AR}}(\tau) = 2I_0 + 2C_{rr}(\tau), \tag{1}$$

where I_0 is a constant and $C_{rr}(\tau)$ is the autocorrelation function of the reflection amplitude $r_g(\tau)$.

To analyze CW-R spectra, standard transfer matrix formalism for multilayered system with planar parallel interfaces has been used. In our case, only three layers will be considered: air, a ZnO dead layer (60 Å), where no exciton exists, and semi-infinite ZnO. The dielectric function of ZnO is expressed as

$$\varepsilon(E) = \varepsilon_b + \sum_{j=A,B}^{N} \int \frac{1}{\sqrt{2\pi}\sigma_j} \frac{f_j}{x^2 - E^2 + i\Gamma_j E} \times \exp\left[-\frac{(x - E_{0j})^2}{2\sigma_j^2}\right] dx, \tag{2}$$

where the background dielectric function ε_b is derived from ellipsometry measurements.[23] In Eq. (2), the following excitonic parameters are considered: homogeneous broadening Γ_j (FWHM), inhomogeneous broadening σ_j (standard deviation), oscillator strength $f_j = 4\pi\alpha_{0j}E_0^2$ (with $4\pi\alpha_{0j}$ the polarisability), and exciton energy E_j of j exciton (j = A, B). The parameter x is the integration variable representing the excitonic resonance of the Gaussian distribution.

In the case of a CW-R simulation, the number of variables that have to be adjusted can affect the accuracy of the values of the latter. To improve the precision, this method has been combined with the AR and Ti-FWM techniques. When two close oscillators are simultaneously excited during the AR experiment, quantum beats are observed. The sharpness of these oscillations depends on the values of oscillator strength. This behavior entails that the combination of CW-R and AR measurements allows then a precise estimation of the oscillator strengths.

In order to investigate the broadening process, Ti-FWM experiments have been carried out. Ti-FWM signal is evaluated by solving the optical Bloch equation within the framework of a two-level system where Coulombian interactions are neglected. The lifetime of the excited state T_1 is assumed to be larger than the dephasing time T_2. Contrary to Yajima,[21] we consider the case when neither homogeneous nor inhomogeneous damping dominates. For positive delay, decay is then written as[24]

$$I_{\mathrm{FWM}}(\tau) = \sqrt{\frac{\pi}{2}} \frac{\exp\left(2/T_2^2\sigma_j^2\right)}{\sigma_j} \exp\left(-\frac{4\tau}{T_2}\right) \times \left[1 + \Phi\left(\frac{\sigma_j}{\sqrt{2}}\tau - \frac{\sqrt{2}}{T_2\sigma_j}\right)\right], \tag{3}$$

where Φ is the error function. In agreement with the previous assumptions, there is no signal for negative delay. The homogeneous broadening Γ can be deduced from the relation $\Gamma = 2\hbar/T_2$.

From Eq. (3), it is straightforward to find two extreme situations where respectively homogeneous or inhomogeneous broadening dominates, as it was done in Ref. 21. In the first case, the relation between the dephasing time T_2 and the experimental decay time T_{dec} is $T_2 = 2T_{\mathrm{dec}}$, whereas in the second case, this relation becomes $T_2 = 4T_{\mathrm{dec}}$. The confrontation of the decay time value derived from Ti-FWM measurements with the broadening parameters deduced from the fitting of CW-R spectra leads to an estimation of both homogeneous and inhomogeneous linewidths. Thus oscillator strength values are determined from the best fit of the CW-R and AR spectra; homogeneous and inhomogeneous damping values are deduced from the combination of the CW-R and Ti-FWM results.

The Ti-FWM spectrum recorded at 5 K is shown in Fig. 1 by a solid black line. The quantum beats observed in the spectrum are induced by the simultaneous excitation of A and B excitons. The measured period corresponds to a splitting ΔE between A and B of 5.5 meV, which is well consistent with previous observation.[7] If one assumes that inhomogeneous broadening is dominant ($\sigma \gg \Gamma$), the measured decay time would be associated to an homogeneous linewidth Γ of 0.5 meV and σ much larger. These parameters do not allow to fit the CW-R spectrum. On the contrary, if the broadening is assumed to be homogeneous ($\Gamma \gg \sigma$), the Ti-FWM decay time corresponds to $\Gamma \sim 1$ meV. In this case, a full agreement is found between calculated and experimental CW-R spectra. An inhomogeneous broadening ($\sigma \sim 0.2$ meV) is added in order to obtain the best agreement between the calculated CW-R spectrum and the experimental one (see Fig. 2). Ti-FWM spectrum is simulated using Eq. (3), where a phenomenological sinusoidal factor is considered in order to account for the beatings. The red line corresponds to the fit (see Fig. 1), and the parameters used for this simulation are listed in Table I (last line). Due to the simultaneous excitation of A and B excitons, an average value of excitonic broadenings

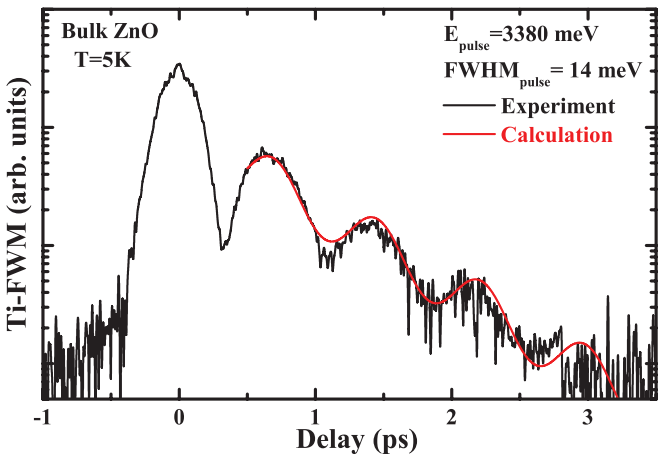

FIG. 1. (Color online) Ti-FWM signal of ZnO bulk sample recorded at 5 K. The pulse energy is 3380 meV, its linewidth is 14 meV, the excitation density per pulse is 0.2 nJ cm^{-2}.

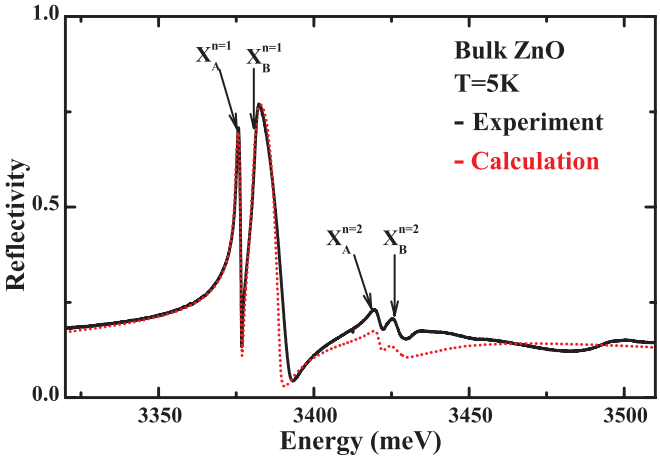

FIG. 2. (Color online) CW-R spectrum of a ZnO bulk sample recorded under normal incidence at 5 K. Solid black line corresponds to the experimental result and red dashed one is the CW-R simulation using a Gaussian local model. The arrows locate the different excitonic transitions.

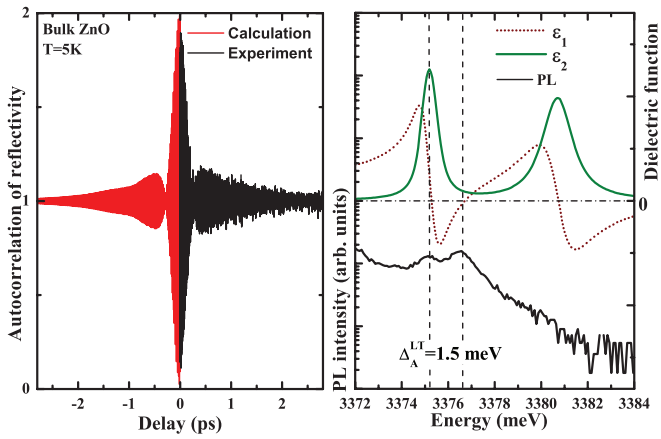

FIG. 3. (Color online) On the left appears the AR spectrum. Results obtained at 5 K with a pulse energy of 3377 meV (black) and calculated (red). Top of right figure, the dielectric function (real and imaginary parts) is plotted to determine the LT splitting of A exciton. At the bottom, the PL spectrum recorded at 5 K. The vertical dashed lines identify transverse and longitudinal modes.

is determined. We assume to be in the range of validity of Eq. (3), and this is well confirmed by the short dephasing time ($T_2 = 1.35$ ps) and the long excitonic lifetime in this kind of high-quality sample ($T_1 > 100$ ps). The dominance of the homogeneous damping in high-quality ZnO contrasts with many bulk semiconductors, e.g., GaAs[25] and GaN,[22] where inhomogeneous broadening prevails at low temperature ($T < 80$ K). It means that the dominant mechanism of exciton scattering in ZnO is the interaction with impurities rather than structural inhomogeneities (dislocations, residual strains, etc.).

Table I contains the parameters used to fit the CW-R spectrum measured at 5 K and those corresponding to the Ti-FWM data. One can see that they are well consistent. To check oscillator strength values, AR data are considered [see Fig. 3(a)], right side in black line]. Their comparison with simulation (left side in red line) is done for the derived excitonic energies and oscillator strength values. The whole set of parameters are validated by the good agreement between experiment data and calculations. Another proof of the reliability of values used for the oscillator strength is given by the splitting between excitonic lines of A excitonic series in a PL spectrum. Two distinct peaks are observed for A exciton; the first one corresponds to the transversal mode and the second to the longitudinal mode.[26] The gap between these peaks should be close to the longitudinal-transverse (LT) splitting (Δ^{LT}) value of A exciton. Indeed, the calculation using the complex dielectric function given by Eq. (2) gives

TABLE I. Excitonic parameters of ZnO obtained at 5 K after a whole analysis including the modelings of Ti-FWM, CW-R, AR, and PL measurements.

	Oscillator strength (meV^2)	$4\pi\alpha_0$	Γ (meV)	σ (meV)	Energy (meV)
XA (CW-R)	155000 ± 5000	0.0136	0.55	0.20	3375.2
XB (CW-R)	250000 ± 5000	0.0219	1.35	0.25	3380.7
$X_{A,B}$ (Ti-FWM)			0.95	0.20	$\Delta E = 5.5$

$\Delta_{\mathrm{A}}^{\mathrm{LT}} = 1.5$ meV that is equal to the experimentally observed energy gap. In Fig. 3(b), the maximum of the imaginary part (ε_2) of the calculated dielectric function gives the transverse mode energy and the longitudinal one is identified by the zero crossing point toward positive values of the real part ε_1.[27] The fact that the LT splitting of A exciton is larger than the linewidth is a proof of the strong exciton-photon coupling; this remark holds also for B exciton. For this reason, optical properties are mainly governed by exciton-polaritons at low temperatures.

Our data evidence a difference between A and B excitonic parameters. Concerning the oscillator strengths, this difference was explained by Wrzesinski[28] owing to symmetry consideration by using twelve-dimensional exciton Hamiltonian. To our knowledge, concerning the homogeneous broadening difference, no explanation has been proposed in the literature. This difference is also observed through Ti-FWM experiments: the deduced dephasing time decreases when the impulsion energy is shifted from A resonance energy to the B one.

Exciton-polariton properties have been extracted at low temperature from the combination of linear (CW-R, AR, PL) and nonlinear (Ti-FWM) spectroscopies. The investigation of the exciton-phonon interaction can be then carried out as a function of temperature (from 5 K to RT), by performing the same previous measurements. Ti-FWM measurements are performed only up to 100 K [see Fig. 4(a)] because the decay time becomes too short with respect to the temporal width of the femtosecond pulse. Broadenings are, however, determined from CW-R spectra [see Fig 4(b)] up to 300 K.

The whole results deduced from CW-R and Ti-FWM experiments are summarized in Fig. 5. The evolution of damping as a function of temperature is modeled by a Segall's law:[29]

$$\Gamma_{\mathrm{tot}}(T) = \Gamma_0 + \Gamma_{\mathrm{ac}} T + \frac{\Gamma_{\mathrm{op}}}{\exp\left(\frac{E_{\mathrm{LO}}}{kT}\right) - 1}. \qquad (4)$$

Here, the constant part (Γ_0), which corresponds to the broadening at 0 K, is mainly due to impurity-exciton scattering. The second term comes from the exciton scattering by

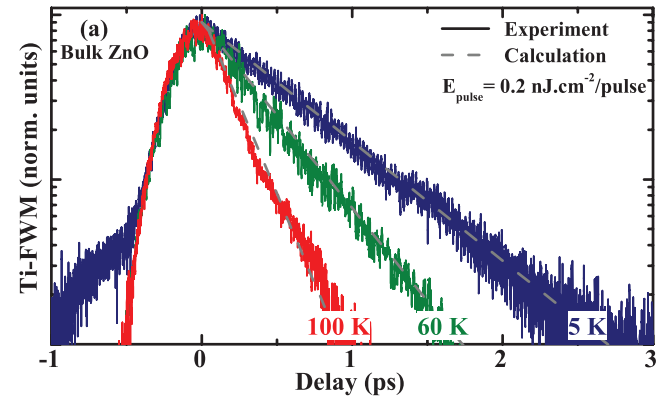

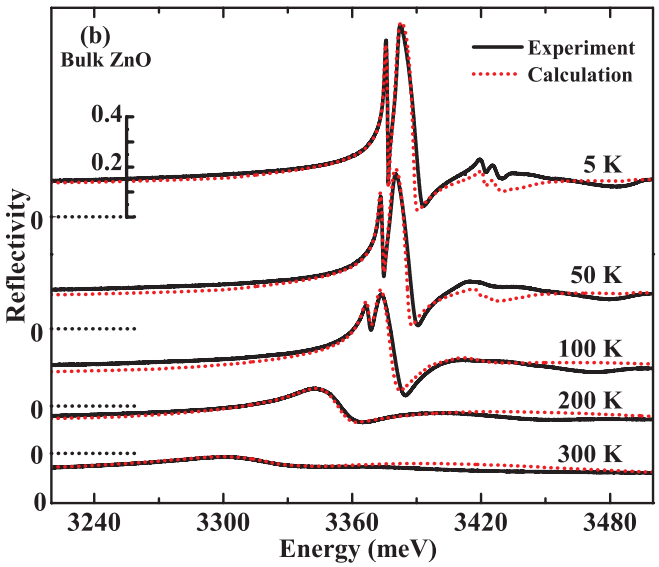

FIG. 4. (Color online) (a) Experimental Ti-FWM (solid line) and the results of calculations using Eq. (3) (dashed line). (b) Temperature dependence of CW-R, in solid black line the experiment and in red dashed line the calculation with a Gaussian local model.

acoustic phonons via both the deformation potential and the piezoelectric interaction. The last term arises from exciton

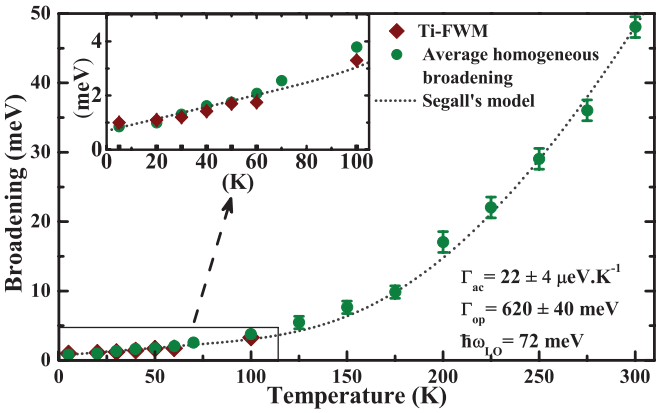

FIG. 5. (Color online) Evolution of homogeneous broadening vs temperature. The average homogeneous broadenings between A and B obtained by Ti-FWM are represented by red lozenges and those achieved from CW-R are reported through green circles. The dashed line is the linewidth evolution following Segall's law.

TABLE II. Set of Segall parameters for different samples.

		Γ_0 (meV)	Γ_{ac} (μeV/K)	Γ_{op} (meV)	E_{LO} (meV)
ZnO	This work	0.8	22	620	72
	Hauschild[12]	0.6[a]	16[a]	47[a]	33
	Hazu[13]	0.25	8.4	14	13
	Makino[20] (XB)	≈8	26.5	783.3	72
GaN	Aoudé[22]	0.1	10	420	91.8
	Korona[30]	1.3	15.3	208	92.3
GaAs	Gopal[25]	0.32	13	30.4	36

[a]Half full width at half maximum reported by the authors.

interactions with longitudinal optical (LO) phonons via the Frölich interaction. Γ_{ac} and Γ_{op} are the exciton-phonon coupling strengths for each type of phonon.

According to literature,[9] the LO phonon energy was fixed to 72 meV; other parameters are deduced from the adjustment to the experimental data. It is found that the exciton-LO phonon interaction in ZnO, characterized by the effective parameter $\Gamma_{op} = 620$ meV is stronger than, e.g., in GaN ($\Gamma_{op} = 400$ meV[22]). This is related to the high polarity of ZnO. The weak exciton-acoustic phonon interaction ($\Gamma_{ac} = 22$ μeV/K) is consistent with the moderate damping increase at low temperature.

The comparison of these values with the published data (see Table II) needs to take into account also the following points: (i) Hauschild *et al.*[12] employ a LO phonon energy different from 72 meV; (ii) the study of Hazu *et al.*[13] was stopped at 70 K, while the exciton-LO phonon coupling is pronounced at high temperature. Only Makino *et al.*[20] report a study up to RT taking a LO phonon energy of 72 meV, but the investigated sample is a thin film and the method employed to deduce the broadening from the width of the absorption features was questionable.[17] Concerning the temperature independent term (Γ_0), its values, 0.4 meV for exciton A and 1.2 meV for exciton B, are comparable to those reported for other high-quality semiconductors, such as GaN[22,30] or GaAs.[25] We can interpret this term through the exciton-impurity scattering only. With the high binding energy of the exciton ($E_b = 61$ meV), the free carrier density is weak even at RT and consequently exciton-free carrier scattering can be neglected. The exciton-exciton scattering is also weak, which was confirmed by the fact that no P band[31] was observed on PL spectrum in the investigated range of excitation densities.

In conclusion, exciton-polariton properties have been investigated in high-quality bulk ZnO crystal from an original approach, which combines linear and nonlinear spectroscopies. In addition to an accurate oscillator strength determination, this analysis allows the separated determination of homogeneous and inhomogeneous broadenings; this determination is extremely tricky with classical methods. This approach is not restricted to ZnO and can be applied to all semiconductors for which accurate knowledge of optical properties is essential to design new optical devices. In our paper, it turns out that, contrary to numerous semiconductors, the broadening in ZnO at low temperature is mainly homogeneous. Temperature-dependent measurements have been also carried out in order to study the exciton-phonon coupling. The analysis of these

data leads to the conclusion that LO phonons interact strongly with excitons and causes significant excitonic broadening at RT.

This work is supported by the European Union under the "Clermont4" project (235114). T.V.S. appreciates the support of the RFBR grant (13-02-00801).

*Corresponding author: emilien.mallet@univ-bpclermont.fr

[1]Z. K. Tang, G. K. L. Wong, P. Yu, M. Kawasaki, A. Ohtomo, H. Koinuma, and Y. Segawa, Appl. Phys. Lett. **72**, 3270 (1998).

[2]M. H. Huang, S. Mao, H. Feick, H. Q. Yan, Y. Y. Wu, H. Kind, E. Weber, R. Russo, and P. D. Yang, Science **292**, 1897 (2001).

[3]S. Chu, M. Olmedo, Z. Yang, J. Y. Kong, and J. L. Liu, Appl. Phys. Lett. **93**, 181106 (2008).

[4]F. Li *et al.*, arXiv:1207.7172 [Phys. Rev. Lett. (to be published)].

[5]F. Medard *et al.*, J. Appl. Phys. **108**, 043508 (2010).

[6]T. C. H. Liew, I. A. Shelykh, and G. Malpuech, Physica E **43**, 1543 (2011).

[7]B. K. Meyer, J. Sann, S. Eisermann, S. Lautenschlaeger, M. R. Wagner, M. Kaiser, G. Callsen, J. S. Reparaz, and A. Hoffmann, Phys. Rev. B **82**, 115207 (2010).

[8]A. Teke, U. Ozgur, S. Dogan, X. Gu, H. Morkoc, B. Nemeth, J. Nause, and H. O. Everitt, Phys. Rev. B **70**, 195207 (2004).

[9]R. Cusco, E. Alarcon-Llado, J. Ibanez, L. Artus, J. Jimenez, B. G. Wang, and M. J. Callahan, Phys. Rev. B **75**, 165202 (2007).

[10]D. G. Thomas, J. Phys. Chem. Solids **15**, 86 (1960).

[11]C. Klingshirn, R. Hauschild, H. Priller, M. Decker, J. Zeller, and H. Kalt, Superlattices Microstruct. **38**, 209 (2005).

[12]R. Hauschild, H. Priller, M. Decker, J. Bruckner, H. Kalt, and C. Klingshirn, Phys. Status Solidi C **3**, 976 (2006).

[13]K. Hazu, T. Sota, S. Adachi, S. Chichibu, G. Cantwell, D. C. Reynolds, and C. W. Litton, J. Appl. Phys. **96**, 1270 (2004).

[14]D. C. Reynolds, D. C. Look, B. Jogai, C. W. Litton, G. Cantwell, and W. C. Harsch, Phys. Rev. B **60**, 2340 (1999).

[15]A. V. Rodina, M. Strassburg, M. Dworzak, U. Haboeck, A. Hoffmann, A. Zeuner, H. R. Alves, D. M. Hofmann, and B. K. Meyer, Phys. Rev. B **69**, 125206 (2004).

[16]M. R. Wagner *et al.*, Phys. Rev. B **80**, 205203 (2009).

[17]C. Klingshirn, R. Hauschild, J. Fallert, and H. Kalt, Phys. Rev. B **75**, 115203 (2007).

[18]M. A. M. Versteegh, D. Vanmaekelbergh, and J. I. Dijkhuis, Phys. Rev. Lett. **108**, 157402 (2012).

[19]T. Takagahara, Phys. Rev. B **31**, 8171 (1985).

[20]T. Makino, C. H. Chia, N. T. Tuan, Y. Segawa, M. Kawasaki, A. Ohtomo, K. Tamura, and H. Koinuma, Appl. Phys. Lett. **76**, 3549 (2000).

[21]T. Yajima and Y. Taira, J. Phys. Soc. Jpn. **47**, 1620 (1979).

[22]O. Aoude, P. Disseix, J. Leymarie, A. Vasson, M. Leroux, E. Aujol, B. Beaumont, A. Trassoudaine, and Y. Andre, Phys. Rev. B **77**, 045206 (2008).

[23]M. Mihailovic *et al.*, Opt. Mater. **31**, 532 (2009).

[24]S. Pau, J. Kuhl, F. Scholz, V. Haerle, M. A. Khan, and C. J. Sun, Appl. Phys. Lett. **72**, 557 (1998).

[25]A. V. Gopal, R. Kumar, A. S. Vengurlekar, A. Bosacchi, S. Franchi, and L. N. Pfeiffer, J. Appl. Phys. **87**, 1858 (2000).

[26]P. Y. Yu, M. Cardona, and L. J. Sham, *Fundamentals of Semiconductors: Physics and Materials Properties* (Springer Verlag, Berlin, 1996).

[27]M. Cobet, C. Cobet, M. R. Wagner, N. Esser, C. Thomsen, and A. Hoffmann, Appl. Phys. Lett. **96**, 031904 (2010).

[28]J. Wrzesinski and D. Frohlich, Solid State Commun. **105**, 301 (1998).

[29]S. Rudin, T. L. Reinecke, and B. Segall, Phys. Rev. B **42**, 11218 (1990).

[30]K. P. Korona, A. Wysmolek, K. Pakula, R. Stepniewski, J. M. Baranowski, I. Grzegory, B. Lucznik, M. Wroblewski, and S. Porowski, Appl. Phys. Lett. **69**, 788 (1996).

[31]C. F. Klingshirn, *Semiconductor Optics* (Springer, Berlin Heidelberg, New York, 2007).